# Model-based 3-D seismic survey design as an optimization problem

*Gabriel Alvarez*, Stanford University, Victor Pereyra and Laura Carcione, Weidlinger Associates.*

## 1 SUMMARY

We present a method that poses the choice of the 3D survey acquisition parameters as an integer optimization problem. We shoot rays from grid points on the target reflector at uniform opening and azimuth angles and record their emergence positions at the surface. An optimization (an exhaustive search in this example) minimizes the distance between the ray emergence coordinates and the source and receiver coordinates of candidate geometries subject to appropriate geophysical and logistics constraints. We illustrate the method with a 3-D subsurface model featuring a target reflector whose depth changes significantly across the survey area and show that, for this model, the standard approach would lead to a design requiring 200 shots/km$^2$ whereas the optimum design requires only 80 shots/km$^2$ without sacrificing the illumination of the target at any depth, or the logistics of acquisition.

## 2 INTRODUCTION

For the design of a 3-D seismic survey to be effective, proper illumination of the target reflector and faults must be achieved. The standard practice of 3-D seismic survey design assumes implicitly that the subsurface is composed of flat layers of constant velocity. Under this assumption, a set of source-receiver geometries have been devised and used extensively (Stone, 1994). These geometries usually correspond to parallel lines of receivers at fixed distances and to parallel lines of sources, also at fixed distances. Input information to the design process is limited to range of target depths and dips, maximum and minimum propagation velocities, and desired fold.

The assumption of flat horizontal layers does not honor the complexity often present in the subsurface in areas of great oil exploration or production interest. The survey designer usually ignores this discrepancy, however, partly because of mistrust of the available subsurface information and partly because of fear that exploiting that information may lead to ineffective logistics or may bias the results. Survey designers often choose the source-receiver geometry from among the few standard geometries available (parallel, orthogonal, slanted, zigzag) on the basis of uniformity of offset and azimuth in the subsurface bins (Galbraith, 1994). Wavefield sampling (Vermeer, 1998) may also be a consideration. In some cases, a 3-D subsurface model obtained from existing 2-D or 3-D data, well logs or geological plausibility is used to compute illumination maps of the reflectors of interest via forward modeling with various candidate geometries (Carcione et. al., 1999; Cain et. al., 1998). The geometry that provides the least distortion in illumination is chosen as the best design.

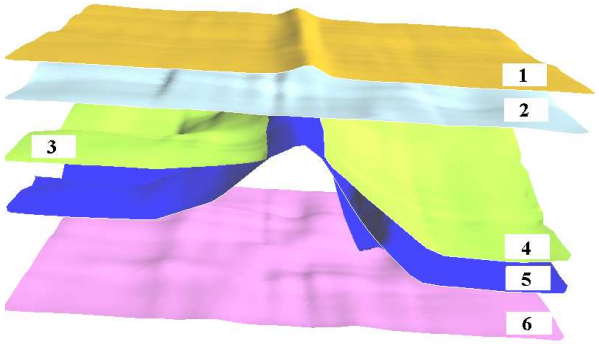


**Figure 1.** Subsurface model. View from the strike direction. The horizontal dimensions are 10 km x 10 km. The depth of the deepest reflector is 3 km.

We propose to pose the selection of the survey parameters as an optimization process that allows the parameters to vary spatially in response to changes in the subsurface. We illustrate the method in 3-D using a subsurface model we created to simulate a land survey. We will show that a standard acquisition geometry will either sacrifice the offset coverage of the shallow part of the target horizon or require a large number of sources, which negatively impacts the cost of the survey. For the sake of simplicity, target depth was the only parameter we allowed to influence the spatial change of the geometry. Three geometries were computed according to the depth of the target reflector. Each geometry was locally optimized for uniformity of subsurface illumination. The optimum geometry, being more flexible, relaxes the acquisition effort without compromising the shallow part of the target reflector.

## 3 SUBSURFACE MODEL

We created a simplified subsurface model corresponding to a target horizon whose depth changes from about 0.3 km to about 2 km. The model simulates a land prospect, has high local dips and mild topography. Figure 1 shows a view of the model from the strike direction. Figure 2 shows a view of the target reflector from the dip direction. The model is 10 km x 10 km with a maximum depth of about 3 km. The velocity field consists of blocks delimited by the reflectors. Within each block the velocity changes laterally as well as vertically in a gradient-based fashion as summarized on Table 1. Velocity at each point of each block is computed as $v(x,y,x) = v_0 + x\frac{\Delta v}{\Delta x} + y\frac{\Delta v}{\Delta y} + z\frac{\Delta v}{\Delta z}$.

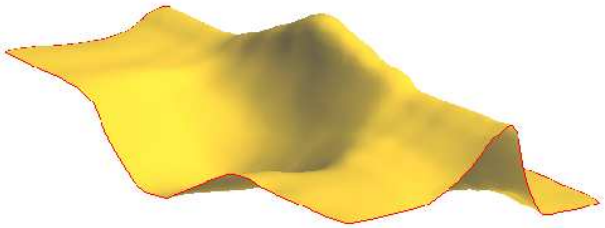

**Figure 2.** Target reflector (number 5 in Figure 1). View from the dip direction. The reservoir corresponds to the top of the structure at a depth of about 0.3 km.

**Table 1.** Velocity information (m/s). Each block is delimited by two reflectors, numbered as indicated on Figure 1.

| Block | Reflectors | $v_0$ | $\frac{\Delta v}{\Delta x}$ | $\frac{\Delta v}{\Delta y}$ | $\frac{\Delta v}{\Delta z}$ |
|---|---|---|---|---|---|
| 1 | 1 and 2 | 2000 | 0.01 | 0.05 | 0.5 |
| 2 | 2 and 3 | 3000 | 0.05 | 0.01 | 0.2 |
| 3 | 3 and 4 | 2400 | 0.01 | 0.01 | 0.5 |
| 4 | 4 and 5 | 3600 | 0.05 | 0.01 | 0.1 |
| 5 | 5 and 6 | 5000 | 0.0 | 0.0 | 0.0 |

## 4 STANDARD 3-D SURVEY DESIGN

Table 2 shows the input data for the standard design. The two most critical parameters, since they control the cost of the survey, are the maximum dip and the minimum target depth. The maximum dip controls the spatial sampling whereas the minimum target depth controls the separation between the receiver and shot lines. Table 3 shows the parameters for a standard design.

Figure 3 shows that there is a problem with the parameters of the standard design: the shortest offset in the central bin is approximately 700 m, which is too large compared to the depth of the shallowest part of the target reflector. The central bins will not have offsets short enough to image the shallow part of the target reflector. Since this is the main target, its image cannot be compromised. In order to decrease the maximum minimum offset we need to decrease the source line interval, the receiver line interval or both. In this particular case, we can simply halve them so that the maximum minimum offset is now just over 300 m. Obviously, halving the *dsl* doubles the number of required shots which in turn may double the cost of the survey. Furthermore,

**Table 2.** Input to the standard design.

| $V_{\min}$ (m/s) | $\theta$max (degrees) | $f$max (Hz) | $z_{\min}$ (m) | $z$max (m) | $fold$ |
|---|---|---|---|---|---|
| 2000 | 60 | 60 | 300 | 3000 | 24 |

**Table 3.** Parameters of the standard design: *dr* is the receiver interval, *ds* is the source interval, *drl* is the receiver line interval, *dsl* is the source line interval, *nchl* is the number of channels per line and *nrl* is the number of receiver lines in the recording patch. All distances in meters.

| *dr* | *ds* | *drl* | *dsl* | *nchl* | *nrl* |
|---|---|---|---|---|---|
| 20 | 20 | 400 | 500 | 150 | 8 |

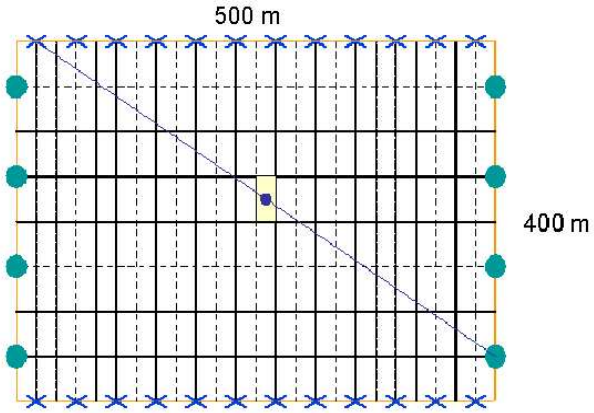


**Figure 3.** Recording box. Receivers are along the horizontal lines and sources along the vertical lines. The minimum possible offset for the bins in the middle of the box is of the order of 700 m, much too large to image the target reflector at 300 m depth.

if the number of active receiver lines is kept constant (which may be necessary if not enough equipment is available) the aspect ratio will also double, making the survey highly azimuthal. A possible solution is to use rectangular bins with the source interval equal to twice the receiver interval. This keeps both the number of shots and the aspect ratio constant, but may be an undesirable solution if significant dips are present in the strike direction (assuming that the source lines are in the strike direction).

## 5 OPTIMIZED 3-D SURVEY DESIGN

Our approach avoids the compromises between the imaging of the shallow reflector and the source density by posing the design as an optimization problem in which the requirements of image quality and the survey cost are balanced within the constraint of sound acquisition logistics. The compromises in the standard design stem from insufficient input data, i.e. an inappropriate subsurface model.

If we can accurately establish the correspondence between the subsurface area of the shallow reflector and

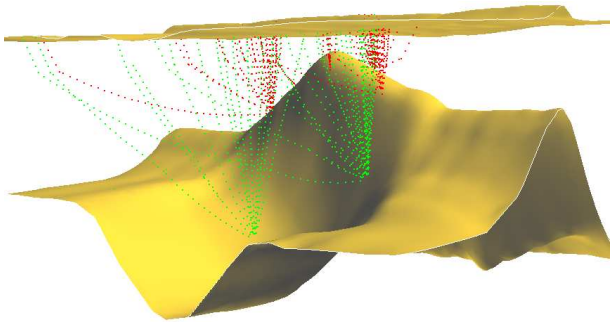

**Figure 4.** Exploding reflector rays. Rays from a few of the reflecting points on the target horizon. There are several thousand such reflecting points, so the resulting density of rays is very large.

the part of the surface area whose sources and receivers contribute to its image, then we could use dense acquisition parameters in that part of the survey area and use more standard parameters elsewhere. A similar approach can be used to locally increase the offsets for high-dipping reflectors, or to increase the azimuth coverage of a locally fractured reservoir.

Using GOCAD, we created a stratigraphic grid of 25 x 25 m draped around the target reflector and used the subsurface model to trace 20 rays from each grid point using the INTEGRA software. The rays were traced at azimuths from 0 to 135 degrees in intervals of 45 and opening angles from 0 to 60 degrees in intervals of 15 degrees. The emergence points of all the rays at the surface were recorded along with other ray tracing information. Figure 4 shows a few of the rays.

If we could make the positions of sources and receivers correspond to the emergence positions of the rays we would have perfect target illumination, to the extent that the subsurface model is accurate. Obviously, in practice there are severe limitations to the geometries we can actually use. We will illustrate the optimization with the simplest, least ambition goal: to divide the acquisition surface into three, possibly overlapping regions, corresponding to the emergence positions of the normal rays from three ranges of target depths. The first range corresponds to the shallowest reflector depth 300 - 400 m. The second range to depths between 400 and 700 m and the third range for depth greater than 700 m. For each of these target-depth ranges we will compute the optimum geometry from among a set of candidate orthogonal geometries summarized on Table 4.

The objective function for the nonlinear integer optimization has two components: one to minimize target illumination irregularity and one to guarantee that the geophysical and logistical constraints are honored.

**Table 4.** Parameters for trial geometries in each zone. Units are in meters.

| Zone | *drl*, *dsl* | *nrl* |
|---|---|---|
| 1 | 180,200,220,240,260,280,300,320 | 6,8,10,12 |
| 2 | 360,380,400,420,460,500,540,580 | 4,6,8,10 |
| 3 | 540,560,580,600,640,680,720,760 | 4,6,8,10 |

$$f_i = (1-\lambda)\sum_{j=1}^{m}\delta_j o_{ij} + \lambda\sum_{j=1}^{n}\epsilon_j c_{ij}, \qquad (1)$$

where $i$ is the index that represents every trial geometry, $\lambda$ is the factor balancing the two contributions to the objective function, $m$ is the number of objectives, $o_{ij}$ is the figure of merit of the $j$th objective for the $i$th geometry, $\delta_j$ is the relative weight of the $j$th objective, $n$ is the number of constraints, $\epsilon_j$ is the relative weight of the $j$th constraint and $c_{ij}$ is the figure of merit of the $j$th constraint for the $i$th geometry. In this case we chose $\lambda = 0.5$ thus giving equal weight to the minimization of the objectives and to the satisfaction of the constraints.

The main objective, as mentioned before, is uniformity of target illumination, which requires minimization of the total distance that the emergence ray positions had to be moved to conform with each geometry. Also, since this is a land survey, the main factor in the cost of the survey is the number of shots. Therefore, we used the minimization of the number of shots as the second objective of the optimization. We also used the total receiver- and source-line cut as an additional, though less important, objective.

As constraints we applied maximum-minimum offset, number of available channels in the recording equipment, survey aspect ratio and surface fold of coverage (Table 5). These constraints are not linear and may be partially fulfilled with partial penalties applied. The figures of merit assigned to the objectives and the constraints are normalized between 0 and 1, except when a constraint is completely violated, for example if the required number of channels is larger than the maximum number of available channels. The relative weights on each objective and on each constraint for the three zones are summarized on Table 6.

## 6 RESULTS

We tried a total of 4608 geometries for each zone with parameter values as summarized on Table 4. Since the search space is small, we used an exhaustive search technique. In more ambitious applications of the method, with more irregular geometries that change spatially in response to the changes in the subsurface we use a micro-genetic algorithm to do the optimization.

**Table 5.** Constraints applied in each zone: $c_1$ is for maximum minimum offset, $c_2$ is for available channels, $c_3$ is for aspect ratio, and $c_4$ is for fold.

| Zone | $c_1$ | $c_2$ | $c_3$ | $c_4$ |
|---|---|---|---|---|
| 1 | 300-400 | 2000,3000,5000 | 1-3 | 24-36 |
| 2 | 500-600 | 2000,3000,5000 | 1-3 | 24-36 |
| 3 | 800-900 | 2000,3000,5000 | 1-2 | 24-32 |

**Table 6.** Weights for the objectives and constraints applied in each zone: $\delta_1$ is for illumination, $\delta_2$ is for the number of shots, $\delta_3$ is for receiver- and source-line cut, $\epsilon_1$ is for maximum-minimum offset, $\epsilon_2$ is for number of available channels, $\epsilon_3$ is for aspect ratio and $\epsilon_4$ is for fold of coverage.

| Zone | $\delta_1$ | $\delta_2$ | $\delta_3$ | $\epsilon_1$ | $\epsilon_2$ | $\epsilon_3$ | $\epsilon_4$ |
|---|---|---|---|---|---|---|---|
| 1 | 0.7 | 0.25 | 0.05 | 0.4 | 0.2 | 0.3 | 0.1 |
| 2 | 0.6 | 0.3 | 0.1 | 0.3 | 0.2 | 0.3 | 0.2 |
| 3 | 0.6 | 0.3 | 0.1 | 0.1 | 0.4 | 0.2 | 0.3 |

Table 7 shows the survey parameters obtained with the exhaustive search in each of the three zones. The parameters are significantly different, especially between zone 1, corresponding to the shallow part of the target horizon, and zone 3 corresponding to the deep part of the same horizon. Notice that having these different parameters does not in itself compromise the logistics, since the distance between the receiver lines in zones 1 and 2 is half that in zone 3. Logistically, all that would be required is to add an additional receiver line between two adjacent receiver lines in zones 1 and 2 assuming that we have enough equipment (and we do, since that was a constraint to the inversion). The different separation of the source lines is even less of a problem since we can in principle drill the shot-holes along any line we want.

The bottom line in terms of cost of the survey, is that the standard dense geometry requires 200 shots/km$^2$ (50 shots/km and 4 receiver lines/km). For this model (100 km$^2$), this means 20000 shots which is extremely high. The optimum design uses the dense parameters 156 shots/km$^2$ (50 shots/km and 3.125 receiver lines/km) only in zone 1, whose area is about 3.5 km$^2$; uses the intermediate design of 148 shots/km$^2$ (50 shots/km and 2.95 receiver lines/km) only in zone 2 whose area is about 7.5 km$^2$; and uses the sparse geometry of 70 shots/km$^2$ (50 shots/km and 1.38 receiver lines/km) in the remaining 89 km$^2$. This gives a total of about 8000 shots, less than half those of the standard geometry. This saving in the number of shots is obtained without compromising the image of the target reflector at any depth and without significantly upsetting the logistics of the acquisition.

**Table 7.** Parameters for the optimum geometry in each zone. Units are meters.

| Zone | $dr$ | $ds$ | $drl$ | $dsl$ | $nrl$ |
|---|---|---|---|---|---|
| 1 | 20 | 20 | 180 | 320 | 12 |
| 2 | 20 | 20 | 360 | 440 | 10 |
| 3 | 20 | 20 | 720 | 720 | 10 |

## 7 CONCLUSION

We have illustrated our methodology for flexible survey design with a very simple example in which a shallow reflector required a particularly dense acquisition geometry and have shown that it is possible to reduce considerably the number of sources by concentrating the acquisition effort where it is really required and relaxing it where is it safe to do so. Similar optimizations are possible for targets whose dip changes rapidly or in situations in which the complexity of the wavefield makes uniformity of the surface locations of shots and receivers detrimental to the illumination of the subsurface targets.

## 8 ACKNOWLEDGMENTS

We would like to thank the sponsors of the Stanford Exploration Project for their support to carry out this study.

## References

Cain, G., Cambois, G., Gehin, M and Hall, R. 1998. Expanded Abstracts. Reducing risk in seismic acquisition and interpretation of complex targets using a GOCAD-based 3-D modeling tool. 68th Annual Internat. Mtg. Soc. of Expl. Geophys. 2072–2075.

Carcione, L., Pereyra, V., Munoz, A., Ordaz, F., Torres, R., Yanez, E. and Yibirin, R. 1999. Model-based simulation for survey planning and optimization. Expanded Abstracts. 69th Annual Internat. Mtg. Soc. of Expl. Geophys. 625–628.

Galbraith, M. 1994. Land 3-D survey design by computer. Austr. Soc. Expl. Geophys. **25**, 71-78.

Stone, D. 1994. Designing Seismic Surveys in Two and Three Dimensions. Society of Exploration Geophysicists.

Vermeer, G. 3-D Symmetric Sampling. Geophysics. **63**, 1629-1647.